(*1*) was extracted repeatedly with dilute sodium hydroxide to remove substances (related to humic acid) of different specific activity in radiocarbon than the native collagen. Due to the size of the Megatheriidae bone, sufficient collagen was prepared which, after burning, filled the proportional counter to 80 percent with pure carbon dioxide (*10*). Subsequently this gas was counted for three separate periods of 2800, 1300, and 1200 minutes each, corresponding to ages of 14,180, 14,150, and 14,080 years. The final weighted composite date was calculated to be 14,150 ± 180 years (UCLA 1464) (*11*).

The date for the moment is the oldest radiocarbon date determined for South America, for which a case can be made involving direct association of man and megafauna. Further, the date is on a humerus from Zone H, the latest of the three zones with the remains of man, so older dates should be forthcoming. If man was well south in the Andes of South America by at least 13,000 B.C., when did he first enter South America?

R. S. MACNEISH
Robert S. Peabody Foundation for Archaeology, Box 71, Andover, Massachusetts

R. BERGER, REINER PROTSCH
Institute of Geophysics and *Departments of Anthropology* and *History, University of California, Los Angeles 90024*

References and Notes

1. R. Berger, A. G. Horney, W. F. Libby, *Science* **144**, 999 (1964).
2. R. S. MacNeish, *ibid.* **143**, 3609 (1964); ———, in *The Prehistory of the Tehuacan Valley*, D. S. Byers, Ed. (Univ. of Texas Press, Austin, 1967), vol. 1.
3. ———, *First Annual Report of the Ayacucho Archaeological-Botanical Project* (Robert S. Peabody Foundation for Archaeology, Andover, Mass., 1969).
4. E. P. Lanning of Columbia University was kind enough to show me his Exacto collection and discuss its relations to the Ayacucho remains.
5. E. P. Lanning, *Burin Industries in the Pleistocene of the Andes*, speech at San Pedro de Atacama, Chile, Dec. 1969.
6. A. Krieger, in *Prehistoric Man in the New World*, J. D. Jenning and E. Norbeck, Eds. (Univ. of Chicago Press, Chicago, 1964).
7. C. Chaud, *Univ. Alaska Anthropol. Pap.* **10**, No. 2 (1963). Also, for earlier similar views see E. N. Wilmsen [*Amer. Antiquity* **29**, No. 3 (1964)] or R. S. MacNeish, *Anthropologica* **1**, (1959)].
8. R. Hoffstetter, "Caractères ancestraux et phylogénie des édentés xénarthes," in *Problèmes Actuels de Paléontologie* (Coll. Int. Centre Nat. Recher. Sci., No. 60, Paris, 1956).
9. T. Y. Ho, L. F. Marcus, R. Berger, *Science* **164**, 1051 (1969).
10. R. Berger and W. F. Libby, UCLA date lists in *Radiocarbon*.
11. ———, *Radiocarbon*, in press.
12. We thank F. Johnson and W. F. Libby for their interest and encouragement. Supported by NSF grant GA 4349.

24 December 1969; revised 24 February 1970

Shear Dependence of Effective Cell Volume as a Determinant of Blood Viscosity

Abstract. *The viscosity of suspensions of human erythrocytes (normal cells in plasma, normal cells in Ringer's solution containing albumin, and hardened cells in Ringer's solution containing albumin) was measured over a wide range of shear rates, and the macrorheological data were correlated with the microrheological behavior of erythrocytes and rigid particles. The formation of rouleaux increases the effective volume of erythrocytes as a result of (i) the increase in axial ratio and (ii) the limitation of deformation of individual erythrocytes. The effective cell volume is the fundamental determinant of blood viscosity.*

The anomalous behavior of blood viscosity, that is, its dependence on shear rate (*1*), has received the increasing attention of investigators in biomedicine, biophysics, and bioengineering. The shear thinning of blood viscosity can be attributed mainly to the shear-dependent deformation and aggregation of red blood cells (RBC) (*2*). Investigations on the microrheological behavior of suspensions have supplied fundamental information on the shear-dependent behavior of particles in suspensions (*3, 4*). By correlating such information with macrorheological data, I show that RBC aggregation and RBC deformation may exert their rheological effects through a common mechanism—namely, shear-dependent changes in the effective cell volume.

Viscosity was determined in a coaxial cylinder viscometer (*2*) over a shear rate range of 500 to 0.01 sec^{-1} at 37°C. Blood was obtained from healthy human subjects. The suspensions included normal RBC in heparinized plasma, normal RBC in 11 percent albumin-Ringer solution, and hardened RBC in 11 percent albumin-Ringer solution, all adjusted to a cell percentage of 45 percent (hematocrit values corrected for fluid trapping in cell column). The 11 percent albumin-Ringer solution (hereafter referred to as albumin solution) had the same viscosity (1.2 centipoises) as plasma but did not cause RBC aggregation. Hardened RBC were prepared by fixing RBC washed in Ringer in 0.5 percent glutaraldehyde solution (*5*).

At low shear rates (for example, 0.1 sec^{-1}), the viscosity is highest for normal RBC in plasma, lower with hardened RBC in albumin, and lowest for normal RBC in albumin (Fig. 1). With an increase in shear rate, the viscosity decreases for suspensions of normal RBC in both plasma and albumin but not for the hardened RBC in albumin. At shear rates above 10 sec^{-1}, the viscosity values of normal RBC in plasma and in albumin are essentially the same, and both are lower than the values for hardened RBC.

The presence of particles in a suspension causes an increase in viscosity as a result of disturbances in streamlines in the fluid medium (*6*). The degree of disturbance is determined by the effective volume concentration of suspended particles, which includes not only the actual volume of the particles but also a volume of external fluid immobilized hydrodynamically. The volume of external fluid immobilized depends on the axial ratio of the particles and the spatial and temporal alignment of the axes with flow—that is, particle orientation and rotation (*3*). The effective particle volume (V_E) of rigid disks and rods in dilute suspensions is much larger than the true particle volume (V_P) (*3, 7*). The ratio V_E/V_P was plotted on logarithmic coordinates against the axial ratio (R) (Fig. 2). For both the rods ($R > 1$) and the disks ($R < 1$), V_E/V_P decreases as R changes toward unity. When R becomes unity, V_E/V_P should be at a minimum and probably is near 1.5, the approximate value for rigid spheres (*8*).

Hardened RBC are rigid discoids with R equal to approximately 0.25 (2 by 8 μ); hence the V_E/V_P value is approximately 2.5 (Fig. 2). Since the

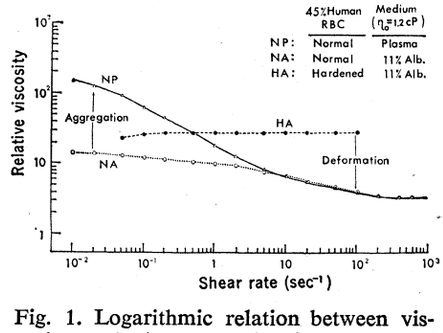

Fig. 1. Logarithmic relation between viscosity and shear rate in three types of suspensions, each containing 45 percent human RBC by volume. Each point represents the mean of four to six experiments. The standard deviations are less than 5 percent of the means.

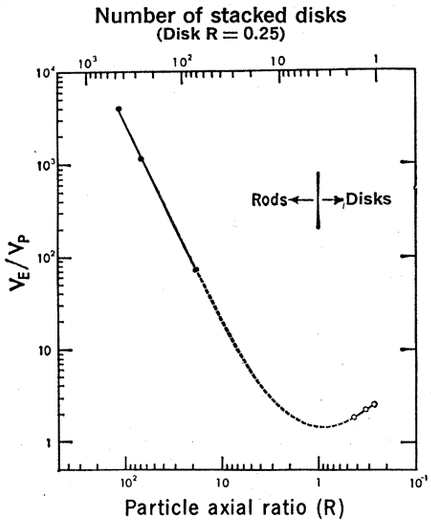

Fig. 2. Logarithmic relation between the ratio of effective particle axial ratio (R, bottom abscissa) in dilute suspensions of rigid rods and disks. The points were taken from the data reported by Mason and his co-workers (*3*, *7*). Extrapolations are made toward a minimum V_E/V_P value of approximately 1.5 at an axial ratio 1.0. Stacking of disks causes an increase in axial ratio and a transformation into rods. The top abscissa shows the number of stacked disks with individual axial ratio of 0.25.

axial ratio and orbiting of rigid particles do not vary with shear, this V_E/V_P ratio is constant at all shear rates (Fig. 3). Under conditions of low shear, the essentially undeformed normal RBC in albumin assume the shape of biconcave discoids and are probably similar to hardened RBC with respect to their V_E/V_P values. With increases in shear rate, however, deformation is induced in the normal RBC, which are comprised of an internal fluid enveloped by a flexible membrane (*4*, *9*). The alignment of the deformed RBC with flow (*4*) reduces the volume of external fluid immobilized and decreases the disturbance of external streamlines. Furthermore, at high shear rates the flexible membrane transmits the shear stress to the internal fluid, which then participates in the flowing streamlines (*4*). Therefore, the V_E/V_P value of normal RBC in albumin decreases with increasing shear and reaches a minimum level with the occurrence of maximum deformation at very high shear rates (Fig. 3). This shear dependence of the V_E/V_P of normal and hardened RBC in albumin (Fig. 3) are in agreement with the shear dependence of their viscosity values (Fig. 1).

The difference between normal RBC in plasma and normal RBC in albumin is primarily the presence of RBC aggregation in the plasma, but there is also a reduction in deformability when aggregations are formed. At low shear rates, normal RBC in plasma form extensive aggregates (*4*), and the rouleaux rotate with little bending (*3*). The stacking of 30 RBC into a long rouleaux ($R \cong 7.5$) causes an increase in V_E/V_P to approximately 10 from the value of approximately 2.5 for the monodispersed RBC (Fig. 2). With increases in shear rate the rouleaux are progressively dispersed (*4*), and they also become more flexible (*3*). Therefore the V_E/V_P decreases (Fig. 3). Although the partially dispersed rouleaux are capable of bending under shear (*3*), their deformability is limited in comparison to the monodispersed normal RBC. If the deformability were the same, the V_E/V_P of four-cell rouleaux ($R \cong 1$) would have been smaller than that of monodispersed RBC ($R \cong 0.25$) (Fig. 2). The higher deformability of the monodispersed normal RBC, however, may compensate for this difference in R. Hence V_E/V_P may be similar for the normal RBC in plasma with small rouleaux and for the monodispersed normal RBC in albumin. Indeed, the viscosity of normal RBC in plasma is nearly identical to that of normal RBC in albumin at shear rates above 10 sec^{-1} (Fig. 1), although a shear rate of at least 50 sec^{-1} is required to disperse all aggregates (*4*). Therefore, at shear rates from 10 to 50 sec^{-1}, the similarity in the macrorheological data between normal RBC in plasma and normal RBC in albumin (Fig. 1) reflects the equivalence of V_E/V_P values resulting from compensating effects of differences in axial ratio and deformability (Fig. 3). When the shear rate is raised above 200 sec^{-1}, the aggregates are completely dispersed, and the normal RBC in plasma and normal RBC in albumin are then equal not only in their macrorheological property but also in their microrheological behavior (degrees of dispersion, deformation, and orientation).

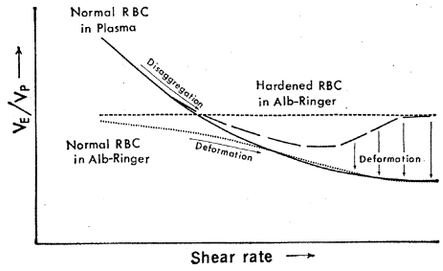

Fig. 3. A semiquantitative plot (without numerical scales) between the ratio of effective cell volume to actual cell volume (V_E/V_P) and the shear rate for three types of erythrocyte suspensions. As a result of the constancy of axial ratio and orbiting, hardened RBC in albumin (broken line) have an essentially constant V_E/V_P. The V_E/V_P value of normal RBC in albumin (dotted line) is close to that of hardened RBC at low shear rates, but it decreases progressively to a constant, low level with increasing shear deformation. The V_E/V_P of normal RBC in plasma (solid line) is highest at low shear rates and decreases with shear disaggregation. If disaggregation were not accompanied by deformation, V_E/V_P of normal RBC in plasma would have followed the upward course indicated by the interrupted solid line (Fig. 2). However, the simultaneous occurrence of shear deformation (the downward arrows) with shear disaggregation prevents this upswing of V_E/V_P and renders it equal to that of normal RBC in albumin.

The results show parallel changes in the shear dependences of viscosity (Fig. 1) and the V_E/V_P values (Fig. 3). The V_E/V_P values in Fig. 2 were obtained on dilute suspensions in which free rotation of particles can occur. At high concentrations (for example, 45 percent RBC), when orbiting is limited by particle crowding, axial alignments exhibit mainly spatial distribution (orientation) rather than temporal variations (rotation). However, the general relation between the V_E/V_P value and the axial ratio may still be similar to that in Fig. 2, since the pattern of spatial distribution of axial alignment is analogous to that of temporal variations (*7*).

I propose that the shear dependence of blood viscosity is the result of a shear dependence of the effective cell volume. Since the effective cell volume is a function of RBC aggregation, RBC deformability, shearing condition, and RBC volume concentration, the variations of blood viscosity with plasma protein concentration, hematocrit, and shear rate can all be explained on a unified basis of the change in effective cell volume.

SHU CHIEN

Laboratory of Hemorheology,
Department of Physiology,
Columbia University College of
Physicians and Surgeons,
New York 10032

References and Notes

1. A. L. Copley and G. Stainsby, Eds., *Flow Properties of Blood and Other Biological Systems* (Pergamon, New York, 1960); L. Dintenfass, *Circulation Res.* **11**, 233 (1962); R. E. Wells, Jr., *N. Engl. J. Med.* **270**, 832 and 889 (1964); M. I. Gregersen, in *Les Concepts de Claude Bernard sur le Milieu Intérieur* (Masson, Paris, 1967), p. 231; E. W. Merrill, *Physiol. Rev.* **49**, 863 (1969).
2. S. Chien, S. Usami, H. M. Taylor, J. L. Lundberg, M. I. Gregersen, *J. Appl. Physiol.* **21**, 81 (1966); S. Chien, S. Usami, R. J. Dellenback, M. I. Gregersen, *Science* **157**, 827 (1967); S. Chien, S. Usami, R. J. Dellenback, M. I. Gregersen, L. B. Nanninga, M. M. Guest, *ibid.*, p. 829; S. Chien, *Advan. Microcirculation* **2**, 89 (1969).
3. H. L. Goldsmith and S. G. Mason, in *Rheology*, F. R. Eirich, Ed. (Academic Press, New York, 1967), vol. 4, p. 86.
4. H. Schmid-Schoenbein, P. Gachtgens, H. Hirsch, *J. Clin. Invest.* **47**, 1447 (1968); H. Schmid-Schoenbein and R. E. Wells, *Science* **165**, 288 (1969).
5. R. M. Widmark, *Technicon Quart.* **1**, 13 (1969).
6. G. I. Taylor, *Proc. Roy. Soc. (London) Ser. A* **146**, 501 (1934).
7. E. Anczurowski and S. G. Mason, *J. Colloid Interface Sci.* **23**, 533 (1967).
8. M. Mooney, *J. Colloid Sci.* **6**, 162 (1951).
9. L. Dintenfass, *Angiology* **13**, 333 (1962); Y. C. Fung, *Fed. Proc.* **25**, 1761 (1966); C. R. Cokelet and H. J. Meiselman, *Science* **162**, 275 (1968).

10. Carried out under Army contract DA-49-193-MD-2272 and supported by PHS research grant HE-06139 and by several private donors, including the Scaife family of Pittsburgh and Mrs. George W. Perkins.

26 January 1970; revised 6 April 1970 ■

Melatonin Synthesis: Adenosine 3′,5′-Monophosphate and Norepinephrine Stimulate N-Acetyltransferase

Abstract. *Treatment of cultured rat pineal glands with norepinephrine or dibutyryl adenosine 3′,5′-monophosphate causes a six- to tenfold stimulation of* N-*acetyltransferase. This enzyme converts serotonin to* N-*acetylserotonin, the immediate precursor of melatonin. The increased synthesis of melatonin caused by norepinephrine treatment appears to be the result of stimulation of* N-*acetyltransferase by an adenosine 3′,5′-monophosphate mechanism.*

Melatonin, the unique pineal methoxyindole, is formed as follows: tryptophan → hydroxytryptophan → serotonin → *N*-acetylserotonin → melatonin (*1*). Studies with intact rat pineals in vitro indicate that melatonin synthesis (*1*) may be controlled by the neurotransmitter norepinephrine (NE) (*2, 3*). The stimulatory effect of this amine might be mediated in part by adenosine 3′,5′-monophosphate (cyclic AMP) (*4–6*), the "second messenger" of many hormones (*7*). These conclusions are based on the following observations. Adenyl cyclase in pineal homogenates and whole pineal glands is stimulated by NE (*4*). The addition of either NE or N^6,O^2-dibutyryl adenosine 3′,5′-monophosphate (dibutyryl cyclic AMP) to pineal gland cultures stimulates the conversion of labeled tryptophan to melatonin (*2, 3, 5, 6*). Cyclic AMP does not produce a similar effect when added to pineal cultures (*5, 6*). This is probably secondary to a slower rate of transport across cell membranes and a more rapid intracellular degradation by a phosphodiesterase (*8, 9*).

The specific metabolic site, or sites, in melatonin synthesis at which the stimulatory effect of NE may be mediated by cyclic AMP (*5, 6*) is not known. No enzyme or transport mechanism in the pineal gland has been observed to be altered after treatment with NE or dibutyryl cyclic AMP.

We report that addition of NE or dibutyryl cyclic AMP to pineal organ cultures results in a six- to tenfold stimulation of net *N*-acetyltransferase synthesis and melatonin production. This indicates that one metabolic site at which the neurotransmitter NE regulates melatonin production through a cyclic AMP mechanism is *N*-acetylation.

Rat pineal glands (*10*) were incubated for 24 hours (*3, 11*). In the first study (Table 1), the incubation medium contained [^{3}H]tryptophan (5 μc/ml, 25 μc/μmole, Schwarz BioResearch). Melatonin production was estimated by measuring the amount of [^{3}H] melatonin that appeared in the incubation medium (*2, 3, 11*). Chloroform extraction (*2, 11*) yielded a radioactive compound that was identified as melatonin by two-dimensional thin-layer chromatography (*12*).

N-Acetyltransferase activity in the homogenate of an individual rat pineal gland or in a portion of a pool of pineal homogenates (*10*) was estimated by measuring the amount of *N*-[^{14}C]acetylserotonin and [^{14}C]melatonin formed by pineal homogenates after incubation with [^{14}C]serotonin (0.5 m*M*) and acetyl coenzyme A (0.5 m*M*) for 30 minutes (*13, 14*).

After the pineal glands were incubated for 8 to 24 hours (Table 1), *N*-acetyltransferase activity in control glands (groups 2 and 3) declined to approximately 30 to 60 percent of the original activity (group 1). Pineal glands incubated in medium containing 1.0 m*M* dibutyryl cyclic AMP (group 4) or 0.1 m*M* NE (group 5) produced six- to tenfold more melatonin during the 16-hour treatment than did control glands (group 3). Homogenates of treated glands had six- to tenfold higher *N*-acetyltransferase activity at the end of culture.

The addition of either 0.1 m*M* NE, 1.0 m*M* dibutyryl cyclic AMP, or 10 m*M* cyclic AMP to enzyme assays of pooled homogenates of cultured control glands or fresh glands did not cause a stimulation of *N*-acetyltransfer-

Table 1. *N*-Acetyltransferase activity and total [^{3}H]melatonin in medium during the last 16 hours of incubation of pineal gland organ cultures. Individual pineal glands were incubated for an initial period of 8 hours, and then transferred to a second culture vessel for an additional 16 hours. Some incubations were stopped at zero time (group 1) and 8 hours (group 2). Control designates that glands were not incubated with drugs. Concentrations of 0.1 m*M* NE, 1.0 m*M* dibutyryl cyclic AMP (DB-cAMP), and 10 μg of cycloheximide (cyclo) per milliliter were present where indicated. *N*-Acetyltransferase activity in homogenates of pineal glands and total [^{3}H]melatonin in the medium from the second culture period were determined at the end of culture. [^{3}H]Melatonin was not detectable in the medium from the first 8-hour incubation, *N*-Acetyltransferase activity is expressed as the number of picomoles of [^{14}C]-serotonin *N*-acetylated per gland per hour. Total [^{3}H]melatonin is expressed as the number of picomoles produced per gland during the last 16 hours of culture. Data are given as mean ± S.E. Number of glands in each group appears in parenthesis. Not detectable, N.D.

Group	Treatment during organ culture		*N*-Acetyltransferase activity	[^{3}H]Melatonin in medium
	Period 1 (0 to 8 hr)	Period 2 (9 to 24 hr)		
1	Not incubated	Not incubated	38.2 ± 13.4 (3)	
2	Control	Not incubated	16.6, 32.3 (2)	
3	Control	Control	14.6 ± 3.1 (6)	86 ± 13 (6)
4	Control	DB-cAMP	159.0 ± 28.8 (3)*	962 ± 21 (3)*
5	Control	NE	88.0 ± 12.2 (3)*	692 ± 11 (3)*
6	Cyclo	Cyclo	14.1 ± 3.3 (3)	N.D.
7	Cyclo	Cyclo + DB-cAMP	34.2 ± 6.1 (3)†	267 ± 27 (3)*
8	Cyclo	Cylco + NE	42.3 ± 2.7 (3)*	69 ± 11 (3)

* Significantly different from group 3, $P \leq .01$. † Significantly different from group 3, $P \leq .05$.